Contrast-enhanced Ultrasound Imaging of Antiangiogenic Tumor Therapy

LAURA V. KLOTZ[1,3], DIRK-ANDRE CLEVERT[2], SIIRI SCHECKINGER[3], SEBASTIAN STRIETH[4] and MARTIN E. EICHHORN[3,5]

[1]*Clinic of General, Visceral, Transplantation, Vascular and Thoracic Surgery, Ludwig-Maximilians-University of Munich, Munich, Germany;*
[2]*Department of Clinical Radiology, University of Munich, Munich, Germany;*
[3]*Walter-Brendel-Centre of Experimental Medicine, University of Munich, Munich, Germany;*
[4]*Department of Otorhinolaryngology, University of Mainz, Mainz, Germany;*
[5]*Department of Thoracic Surgery, University of Heidelberg, Heidelberg, Germany*

Abstract. *Background/Aim: Anti-angiogenic treatment is a promising strategy for cancer therapy and is currently evaluated in clinical trials. The aim of the present study was to further investigate the effects of an anti-angiogenic therapy, inhibiting vascular endothelial growth factor (VEGF) and endothelial growth factor (EGF) using a tyrosine kinase inhibitor for blocking tumor angiogenesis and tumor progression in vivo. Materials and Methods: Experiments were performed using C57/Bl6 mice (25±5 g of body weight (b.w.)) implanted with subcutaneous Lewis lung carcinoma (LLC-1). From day 7 till 21 after tumor cell implantation, animals (n=7 per group) were treated by monotherapy using ZD6474 (50 mg/kg b.w. per os (p.o.)) daily. A control group received only the solvent polysorbate 80. Using contrast enhanced ultrasound (CE-US) parameters of intra-tumoral microcirculation animals were examined 24 h after the last application of ZD6474. Moreover, subcutaneous tumor growth was measured over the whole therapy period. Finally, histological analyses were performed to analyze the functional vessel density in the tumor tissue. Results: ZD6474 reduced tumor growth of LLC-1 in C57/Bl6 mice significantly. A significant difference of maximal signal intensity (ΔSI_{max}) and area below the intensity time curve (AUC) after antiangiogenic therapy was recorded in the tumor center by CE-US. Vessel density after hematoxyline and eosin, as well as CD31, staining showed no significant difference in both groups. Conclusion: Anti-angiogenic effects can be quantitatively demonstrated using CE-US imaging, which represents the spreading of efficient vessels in the tumor tissue, especially in the tumor center.*

Correspondence to: Laura V. Klotz, Clinic of General, Visceral, Transplantation, Vascular and Thoracic Surgery, Klinikum Grosshadern, Ludwig-Maximilians-University of Munich, Marchioninistrasse 15, 81377 Munich, Germany. Tel: +49 89 857910, Fax: +49 89 857914206, e-mail: Laura.Klotz@med.uni-muenchen.de

Key Words: Anti-angiogenic therapy, ZD6474, contrast enhanced ultrasound, vessel density, tumor microcirculation, angiogenesis, imaging.

Angiogenesis, the formation of new blood vessels from the existing vasculature, is indispensable for tumor growth, metastasis and disease progression. Without a network of efficient vessels, nutrition and oxygen cannot be guaranteed for the surrounding tumor tissue. Consequently, the survival of proliferating tumor cells is not possible.

Based on this fact, one of the most promising therapy options concerning cancer therapy is the concept of antiangiogenesis as Judah Folkman postulated in 1971 (1). The tumor vessel network should be destroyed to cause a significant reduction of blood flow, thus leading into a widespread tumor cell death. In this pathway, vascular endothelial growth factor (VEGF) is an important mediator of tumor growth known to have various functions in angiogenesis, vascular permeability and the regulation of endothelial cell proliferation and migration (2). Therefore, vascular endothelial growth factor receptors (VEGFRs) are mainly expressed on vascular endothelial cells and stimulated by VEGF. Currently, three different VEGFRs are described but only VEGFR-1 and VEGFR-2 are supposed to play a key role in the mechanism of angiogenesis and tumor growth (2, 3).

In the last years, anti-angiogenic agents, aimed to inhibit the growth of tumor vasculature, are increasingly developed for the treatment of solid tumors. Solid tumors depend on a functional vessel network for survival and proliferation. Therefore, anti-angiogenic treatment seems to be an important and potential possibility to avoid tumor growth.

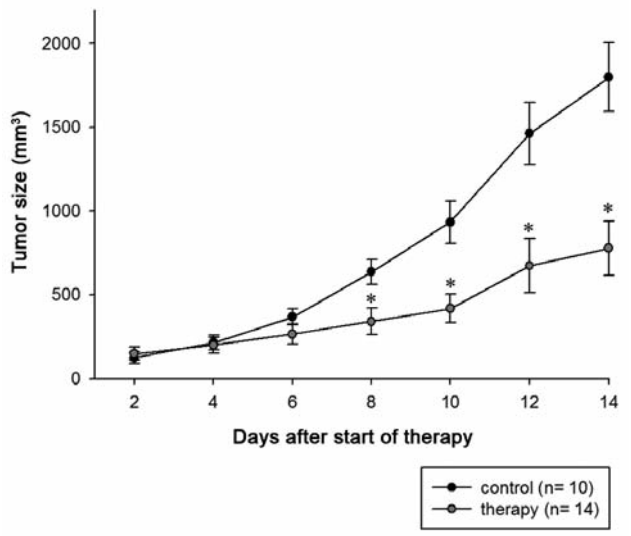

Figure 1. *Tumor size of subcutaneous LLC-1 during anti-angiogenic therapy with ZD6474.*

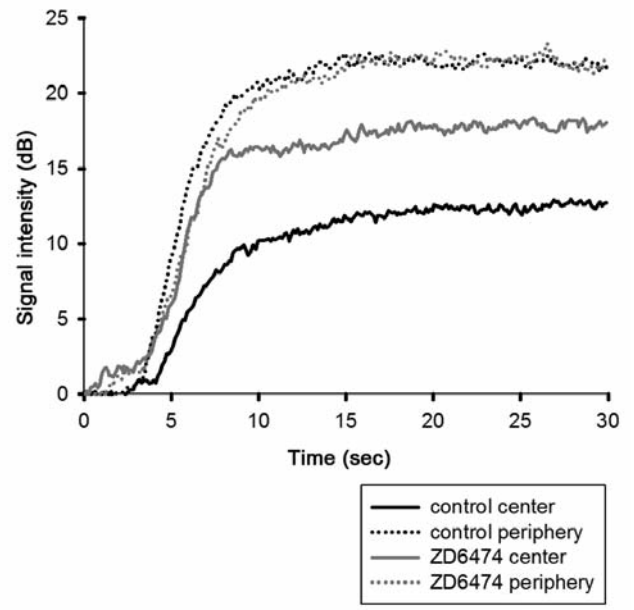

Figure 2. *Intensity-time curves of tumor periphery and tumor center of control tumors (black) and tumors after anti-angiogenic therapy with ZD6474 (red) after measurements using contrast-enhanced ultrasound.*

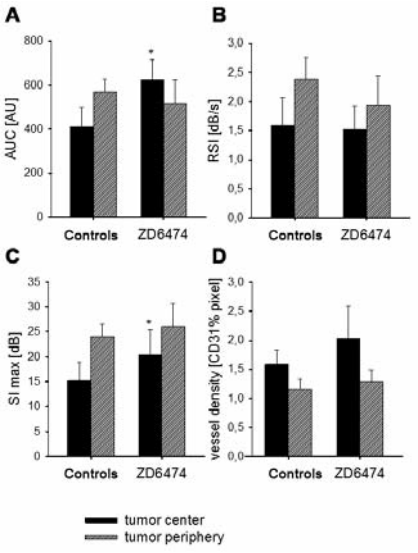

Figure 3. *Contrast enhanced ultrasound (CE-US) imaging and histological results of tumor microcirculation. (A) area under time-intensity curve (AUC), (B) rate of signal increase (RSI), (C) change of signal intensity from baseline to initial peak (ΔSI_{max}) and (D) quantitative analysis of microvessel density (CD31-staining). Results are given as mean±SEM. Significant difference was defined when $p<0.05$.*

ZD6474 is a novel, orally-available VEGFR-2 tyrosine kinase inhibitor, which, additionally, targets epidermal growth factor receptor (EGFR) tyrosine kinase. Both receptors play key roles in the angiogenic pathway of tumor growth. Monitoring the response of tumor tissue to anti-angiogenic treatment by measuring the tumor size should not be the single parameter during anti-angiogenic therapy because tumor cell growth is indirectly suppressed by an insufficient tumor vasculature. To retrace the effects of anti-angiogenic therapy on tumor vasculature and tumor growth in clinical trials, standardized and validated diagnostic methods are necessary to measure changes in the tumor vascular network and vessel function. Hence, several non-invasive imaging methods have already been applied in experimental animal studies, as well as in clinical trials, including dynamic contrast-enhanced magnetic resonance imaging (DCE-MRI), positron emission tomography (PET), contrast enhanced computed tomography (CE-CT) and contrast enhanced ultrasound (CE-US) (4-6).

The intention of the following study was to evaluate CE-US for quantitative assessment of tumor microcirculation during the drug discovery process of antiangiogenic agents. To validate this approach, we measured the effects of ZD6474 on tumor microcirculation *in vivo*. After anti-angiogenic treatment with ZD6474, histological analyses were employed to correlate the morphological tissue modifications to dynamic ultrasound parameters.

Materials and Methods

Animals, tumor model and treatment protocol. After approval by the local ethics committee, experiments were performed on male C57/Bl6 mice (25±5 g of body weight (b.w.)). All experiments were performed in accordance with the United Kingdom Coordinating Committee on Cancer Research (UKCCCR) guidelines for the welfare of animals in experimental neoplasia. The animals were placed in single cages with free access to water and standard laboratory food (Sniff GmbH, Soest,

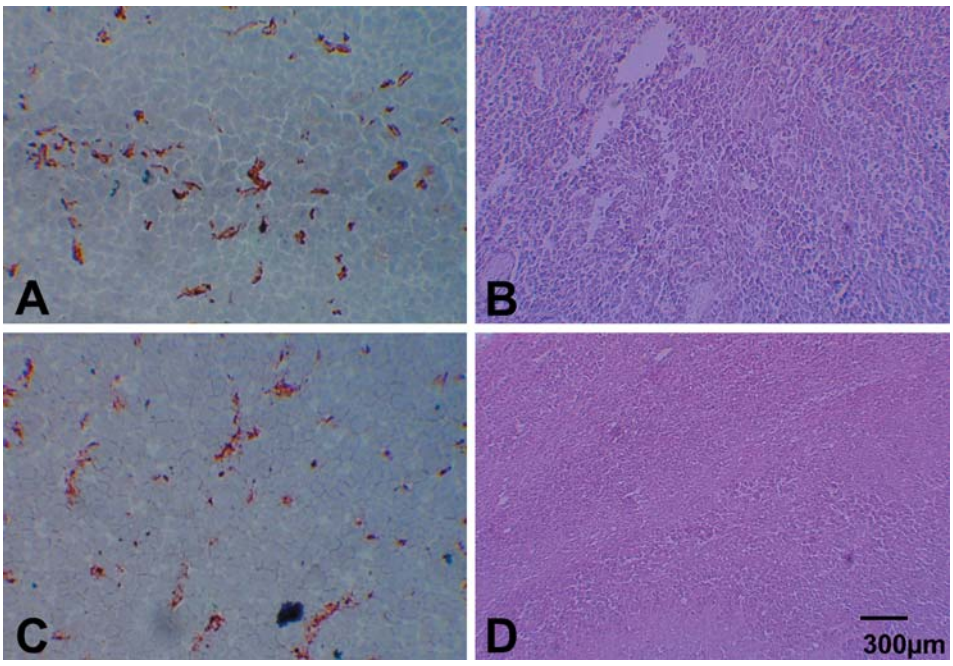

Figure 4. *Histological analysis of subcutaneous LLC-1 carcinomas. Left side with CD31-staining of tumor center (A) and tumor periphery (C) of ZD6474-treated tumors. Right side shows H&E staining of tumor center (B) and tumor periphery (D) of ZD6474-treated tumors.*

Germany) according to institutional and governmental guidelines. All surgical procedures were performed under general anesthesia with ketamine (100 mg/kg b.w. intraperitoneally (*i.p.*), Ketavet®; Parke-Davis, Berlin, Germany) and xylazine (10 mg/kg b.w. *i.p.*, Rompun®; Bayer, Leverkusen, Germany).

Lewis lung carcinoma (LLC-1) cells were cultured in Dulbecco`s modified Eagle's medium (DMEM; Biochrom, Berlin, Germany) supplemented with 10% inactivated fetal bovine serum plus penicillin/streptomycin (Pan Biotech GmbH, Aidenbach, Germany) and incubated in 5% CO_2 at 37˚C.

The dorsal skin of C57/Bl6 mice was shaven and depilated. LLC-1 tumor cells (5×10^6) were suspended in a 10 µl volume DMEM and injected subcutaneously in the dorsal skin. After tumor cell inoculation, the longer (l) and the shorter (b) perpendicular axes and the height (h) of each tumor were measured and tumor volume was calculated according to the following formula:

$$V_{tumor}=l\times b\times h\times {}^{\pi}/_{6}$$

Body weight of animals was measured every other day. ZD6474 was kindly provided by Astra Zeneca (Macclesfield, UK) and was dissolved in a solution of polysorbate 80 (Sigma Aldrich Chemie GmbH, Steinheim, Germany). After 10 days, when subcutaneous LLC-1 tumors were well established, animals were randomised. The treatment group (n=7) received a dose of ZD6474 (50 mg/kg, *per os (p.o.)*) every second day. Control animals (n=7) received polysorbate 80 in an equivalent volume. Ultrasound imaging was performed 24 h after the last treatment.

Contrast enhanced ultrasound. To enable imaging of subcutaneous tumors, mice were anesthetized with 8% inhaled halothane in oxygen and kept under a heat lamp to avoid body temperature reduction. Ultrasound imaging was performed with an Acuson Sequoia 512 machine (Siemens Healthcare, Erlangen, Germany) using a 15L8-MHz multifrequency transducer for all experiments. The Cadence™ contrast pulse sequencing (CPS) technology was used. The detection technique applied the non-linear microbubble energy within the same fundamental frequency band as the transmitted pulse of sound to obtain an improved sensitivity. The mechanical index was lowered to 0.4 or less and the frequency was set to 14 MHz. For examination, mice were placed in the prone position and imaging was performed through a 1 cm gel standoff heated to 37˚C. Imaging depth and focal zone location was adjusted. First, B-mode imaging of the tumors in longitudinal and transverse direction was performed for an adequate measurement of tumor size. Imaging was performed with the second generation contrast agent Sonovue (Bracco, Milano, Italy), which is a stabilised microbubble suspension containing sulphur hexafluoride (SF_6), an echogenic and poorly soluble gas, stabilized in a shell by a monolayer of phospholipids. The mean size of the intravascular remaining particles ranges between 2 to 3 µm. Sonovue was injected as an intravenous bolus (3.5 µl/g b.w.) into the lateral tail vein of each mouse. Imaging was recorded on video shortly before the injection up to two minutes at a frame rate of 8-10 Hz. Injections of the contrast agent were considered adequate if the peak of contrast enhancement was visible within the inferior aorta or the vena cava immediately after the injection. After two minutes of recording, the microbubbles were destroyed by using the destructive imaging method. Afterwards, measurements were repeated by another injection of Sonovue.

All digital data sets were evaluated using the Dicom raw data on the ultrasound machine as a workstation. Three regions of interest

(ROI) were determined in each subcutaneous tumor: the first ROI was drawn around the entire tumor area, another one was marked in the tumor centre and the third one in the tumor periphery. The size of the marked ROI differed depending on the tumor size. Time-intensity curve (TIC) analyses were made offline before the whole data were transferred into a spreadsheet table (Excel 2007; Microsoft, Redmond, WA, USA). The first 30 sec after contrast agent injection were used for further analyses. Initially, each TIC was normalized for precontrast baseline signal intensity (SI). Next, the change in SI from baseline to initial peak (ΔSI_{max}) in decibels, the rate of SI increase from baseline to initial peak (RSI) in decibels per second and the area under time intensity curves (AUC) in arbitrary units were calculated. Two repetitive measurements in each animal were averaged.

Immunohistochemistry. After CE-US imaging, mice were sacrificed and tumors were prepared for further histological investigation. Tissue samples were either fixed in 1% paraformaldehyde and embedded into paraffin for hematoxylin and eosin (H&E) staining or frozen on dry ice for immunohistochemical studies.

Multiple sections of tumor tissue with a thickness of 5 μm were taken from all samples. For the examination of tumor microvessel density, immunohistochemical staining for CD31 (PECAM-1; Santa Cruz, Heidelberg, Germany) was performed. For quantitative analysis, tissue sections were examined using a Zeiss Axiophot 2 microscope (Zeiss, Jena, Germany) fitted with a 20× objective combined with digital image analysis (KS400; Zeiss). Specific CD31 staining was obtained after interactively setting an red, green and blue (RGB)-threshold, which depicts only specific CD31 staining. The vessel density was calculated as percentage of the total area of CD31-positive pixels related to the total image area. A minimum of 15 ROIs from different slides and tumor areas (tumor center and tumor periphery) were randomly selected and analyzed.

Statistical analysis. All results are shown as mean±standard error of the mean (SEM). Statistical analysis of the data sheets were performed using the non-parametric Mann-Whitney rank sum test for intergroup comparison. To analyze the variability of a parameter in the same individual, the Wilcoxon signed rank test was used. All p-values < 0.05 were considered to indicate a statistically significant difference. All analyses were performed with the SigmaStat software (version 3.5; Systat Software Inc., Erkrath, Germany).

Results

Treatment by monotherapy, using ZD6474 (50 mg/kg b.w. *p.o.*) daily, started on day 7 after subcutaneous tumor cell implantation. A significant decrease ($p=0.001$) in tumor size compared to the controls was measured during the treatment period (Figure 1). The averaged signal time-intensity curves corresponding to tumor center and periphery are displayed in Figure 2. In both groups, a mono-exponential increase of contrast-enhancement can be measured after an intravenous bolus injection of microbubbles.

The signal enhancement in tumors treated with ZD6474 compared to control tumors displayed a strong heterogeneity between tumor center and tumor periphery. In the tumor periphery, nearly equal curves were pictured after microbubble injection in both groups. In the tumor center, a higher increase of signal enhancement was measured in the tumors after antiangiogenic therapy compared to control tumors.

Parameters quantified from time-intensity curves corresponding to the tumor periphery and tumor centre are illustrated in Figure 3. Following contrast agent administration, AUC value corresponding to the tumor center was significantly higher in ZD6474-treated tumors compared to control tumors ($p=0.043$). In addition, the value of ΔSI_{max} of the tumor center was significantly higher in treated tumors compared to the controls ($p=0.048$). The RSI value showed no significant difference.

Interestingly, following the application of Sonovue, the values of RSI, ΔSI_{max} and AUC corresponding to the tumor periphery are not significantly different in tumors after antiangiogenic treatment with ZD6474 compared to the control group.

Tumor vessel density, detected between ZD6474-treated tumors and control tumors concerning H&E and immunohistochemical CD31-staining (Figure 4), showed no significant differences for the tumor center ($p=0.093$). Both groups showed nearly similar data respecting the measured vessel density in the tumor periphery ($p=0.867$). Without being statistically significant, histological vessel density showed well-fitting results compared to the described ultrasound parameters.

Discussion

In the present study, we used CE-US imaging with the contrast agent Sonovue to analyze the vascular effects of the anti-angiogenic agent ZD6474. Antiangiogenic therapy should avoid neovascularization by inhibiting new blood vessel formation and should achieve tumor dormancy because tumors depend on a sufficient neoangiogenesis to survive and grow beyond a volume of a few cubic millimetres. By repressing tumor-induced angiogenesis and VEGF-signaling, tumor cell proliferation and tumor expansion should be switched-off depriving the tumor tissue of essential oxygen and nutrients (3, 7, 8). A few years ago, Jain *et al.* suggested that the regular application of antiangiogenic therapy may reverse the abnormal vessel structure of tumor vascularization. Consequently, the vessel network is supposed to be more efficient for the delivery of drugs and oxygen to the existing tumor tissue (8).

ZD6474 is a tyrosine kinase inhibitor of VEGFR-2 and EGFR, which represent essential regulators of endothelial cell proliferation, migration, differentiation and survival. Besides, these growth factors play an important role in tumor angiogenesis (2, 9). Pre-clinical studies have confirmed its anti-angiogenic effects in a wide range of cancer types (9, 10). Phase III clinical studies are underway with applying ZD6474 in non-small cell lung cancer (NSCLC) following promising results in phase II and III studies (3, 9, 11, 12). To evaluate therapy response, an adequate imaging modality is indispensable to monitor anti-angiogenic therapy in

clinical studies, achieve important information about the mechanism of action of these therapeutic agents and optimize this new treatment concept (6, 13, 14).

For the present study, we employed LLC-1, which has been used to study angiogenesis in tumor tissue frequently (5, 15). Implanted subcutaneously in the dorsal skin, LLC-1 cells gave rise to rapidly growing tumors with areas of necrosis and a tortured vascular network (5).

In the present study, we determined the effects of angiogenesis inhibitors on tumor vasculature and tumor growth *in vivo*. The measured significant decrease in tumor growth after treatment with ZD6474 compared to control tumors represents the antiangiogenic effect by inhibiting VEGF signaling, followed by an inhibition of angiogenesis and tumor growth as it is previously described in the literature (16, 17).

We demonstrated that functional therapeutic effects on the tumor microcirculation by anti-angiogenic therapy with ZD6474 can be quantitatively detected by non-invasive CE-US. The measured values of ΔSI_{max} and AUC after antiangiogenic treatment with ZD6474 describe the different tumor vessel network in the therapy group compared to untreated control tumors. In the tumor center, the signal enhancement of tumors after treatment with ZD6474 is overall higher than the enhancement in control tumors. This represents a yielding uptake of contrast medium in the few but efficient-formed tumor vessels after treatment with the antiangiogenic agent (8). Signal enhancement in the tumor periphery is nearly equal in both groups, possibly because of supplemental perfusion by vessels from the surrounding tissue.

The central region of control tumors harbors large areas of necrotic tumor tissue with malfunctioning and confusing vessels of different size because of the fast growing tumor tissue. This illustrates the different types of tumor vessels in larger-growing tumors: Pre-existing normal vessels, mostly dislocated by rapid tumor expansion, supply the peripheral tumor tissue with nutrients and oxygen. Otherwise, newly-formed vessels, with an abnormal vessel structure because of abnormal vascular endothelia, can be detected unequally distributed in the tumor tissue (7, 18). It can be presumed that anti-angiogenic therapy inhibits the formation of new blood vessels and reverses the confuse vessel structure in the tumor tissue to achieve an efficient vascularization in the tumor tissue (19, 20). Referring to the measured parameters of CE-US, it can be hypothesized that this effect is responsible for the significant lower tumor growth and the increased signal enhancement during CE-US imaging.

In addition, histological analysis of the tumor vasculature, characterized by quantitative measurement of microvessel density after CD31 staining, show almost compatible results for both groups. Matching to the functional parameters of CE-US imaging, microvessel density in the tumor center increases in the treatment group after antiangiogenic therapy with ZD6474. This measurement might confirm the hypothesis of numerous, small-sized but well-structured vessels in smaller tumors after antiangiogenic therapy (8).

In summary, we demonstrated the anti-angiogenic effect of ZD6474 using CE-US as an established *in vivo* imaging technology. Due to its clinical availability, non-invasiveness and lack of ionizing radiation, CE-US imaging represents a feasible tool to quantitatively investigate anti-angiogenic effects during the drug discovery process.

References

1 Folkman J: Tumor angiogenesis: therapeutic implications. N Engl J Med *285*: 1182-1186, 1971.

2 Ferrara N, Gerber HP and LeCouter J: The biology of VEGF and its receptors. Nat Med *9*: 669-676, 2003.

3 Doebele RC, Spigel D, Tehfe M, Thomas S, Reck M, Verma S, Eakle J, Bustin F, Goldschmidt J, Jr., Cao D, Alexandris E, Yurasov S, Camidge DR and Bonomi P: Phase 2, randomized, open-label study of ramucirumab in combination with first-line pemetrexed and platinum chemotherapy in patients with nonsquamous, advanced/metastatic non-small cell lung cancer. Cancer Nov 6, doi 10.1002/cncr.29132 , 2014.

4 Rehman S and Jayson GC: Molecular imaging of antiangiogenic agents. Oncologist *10*: 92-103, 2005.

5 Eichhorn ME, Klotz LV, Luedemann S, Strieth S, Kleespies A, Preissler G, Lindner M, Jauch KW, Reiser MF and Clevert DA: Vascular targeting tumor therapy: non-invasive contrast enhanced ultrasound for quantitative assessment of tumor microcirculation. Cancer Biol Ther *9*: 794-802, 2010.

6 Zhang CC, Yan Z, Giddabasappa A, Lappin PB, Painter CL, Zhang Q, Li G, Goodman J, Simmons B, Pascual B, Lee J, Levkoff T, Nichols T and Xie Z: Comparison of dynamic contrast-enhanced MR, ultrasound and optical imaging modalities to evaluate the antiangiogenic effect of PF-03084014 and sunitinib. Cancer Med *3*: 462-471, 2014.

7 Eichhorn ME, Kleespies A, Angele MK, Jauch KW and Bruns CJ: Angiogenesis in cancer: molecular mechanisms, clinical impact. Langenbecks Arch Surg *392*: 371-379, 2007.

8 Jain RK, Tong RT and Munn LL: Effect of vascular normalization by antiangiogenic therapy on interstitial hypertension, peritumor edema, and lymphatic metastasis: insights from a mathematical model. Cancer Res *67*: 2729-2735, 2007.

9 Morabito A, Piccirillo MC, Falasconi F, De Feo G, Del Giudice A, Bryce J, Di Maio M, De Maio E, Normanno N and Perrone F: Vandetanib (ZD6474), a dual inhibitor of vascular endothelial growth factor receptor (VEGFR) and epidermal growth factor receptor (EGFR) tyrosine kinases: current status and future directions. Oncologist *14*: 378-390, 2009.

10 Williams KJ, Telfer BA, Brave S, Kendrew J, Whittaker L, Stratford IJ and Wedge SR: ZD6474, a potent inhibitor of vascular endothelial growth factor signaling, combined with radiotherapy: schedule-dependent enhancement of antitumor activity. Clin Cancer Res *10*: 8587-8593, 2004.

11 Natale RB, Thongprasert S, Greco FA, Thomas M, Tsai CM, Sunpaweravong P, Ferry D, Mulatero C, Whorf R, Thompson J, Barlesi F, Langmuir P, Gogov S, Rowbottom JA and Goss GD: Phase III trial of vandetanib compared with erlotinib in patients with previously treated advanced non-small-cell lung cancer. J Clin Oncol *29*: 1059-1066, 2011.

12 Herbst RS, Sun Y, Eberhardt WE, Germonpre P, Saijo N, Zhou C, Wang J, Li L, Kabbinavar F, Ichinose Y, Qin S, Zhang L, Biesma B, Heymach JV, Langmuir P, Kennedy SJ, Tada H and Johnson BE: Vandetanib plus docetaxel versus docetaxel as second-line treatment for patients with advanced non-small-cell lung cancer (ZODIAC): a double-blind, randomised, phase 3 trial. Lancet Oncol *11*: 619-626, 2010.

13 Lassau N, Chami L, Benatsou B, Peronneau P and Roche A: Dynamic contrast-enhanced ultrasonography (DCE-US) with quantification of tumor perfusion: a new diagnostic tool to evaluate the early effects of antiangiogenic treatment. Eur Radiol *17 Suppl 6*: F89-98, 2007.

14 Zhu XD, Zhang JB, Fan PL, Xiong YQ, Zhuang PY, Zhang W, Xu HX, Gao DM, Kong LQ, Wang L, Wu WZ, Tang ZY, Ding H and Sun HC: Antiangiogenic effects of pazopanib in xenograft hepatocellular carcinoma models: evaluation by quantitative contrast-enhanced ultrasonography. BMC Cancer *11*: 28, 2011.

15 Manegold PC, Hutter J, Pahernik SA, Messmer K and Dellian M: Platelet-endothelial interaction in tumor angiogenesis and microcirculation. Blood *101*: 1970-1976, 2003.

16 Conrad C, Ischenko I, Kohl G, Wiegand U, Guba M, Yezhelyev M, Ryan AJ, Barge A, Geissler EK, Wedge SR, Jauch KW and Bruns CJ: Antiangiogenic and antitumor activity of a novel vascular endothelial growth factor receptor-2 tyrosine kinase inhibitor ZD6474 in a metastatic human pancreatic tumor model. Anticancer Drugs *18*: 569-579, 2007.

17 Gule MK, Chen Y, Sano D, Frederick MJ, Zhou G, Zhao M, Milas ZL, Galer CE, Henderson YC, Jasser SA, Schwartz DL, Bankson JA, Myers JN and Lai SY: Targeted therapy of VEGFR2 and EGFR significantly inhibits growth of anaplastic thyroid cancer in an orthotopic murine model. Clin Cancer Res *17*: 2281-2291, 2011.

18 Fukumura D, Duda DG, Munn LL and Jain RK: Tumor microvasculature and microenvironment: novel insights through intravital imaging in pre-clinical models. Microcirculation *17*: 206-225, 2010.

19 Siemann DW and Horsman MR: Vascular targeted therapies in oncology. Cell Tissue Res *335*: 241-248, 2009.

20 Steeghs N, Rabelink TJ, op 't Roodt J, Batman E, Cluitmans FH, Weijl NI, de Koning E and Gelderblom H: Reversibility of capillary density after discontinuation of bevacizumab treatment. Ann Oncol *21*: 1100-1105, 2010.

Received February 1, 2015
Revised February 8, 2015
Accepted February 10, 2015